POLISH MARITIME RESEARCH 2 (90) 2016 Vol. 23; pp. 42-47
10.1515/pomr-2016-0019

NUMERICAL MODEL OF SO_2 SCRUBBING WITH SEAWATER APPLIED TO MARINE ENGINES

M. I. Lamas[a]
C. G. Rodríguez[a]
J. D. Rodríguez[a]
J. Telmo[b]
[a] University of Coruña. Spain
[b] University of Santiago de Compostela. Spain

ABSTRACT

The present paper proposes a CFD model to study sulphur dioxide (SO_2) absorption in seawater. The focus is on the treatment of marine diesel engine exhaust gas. Both seawater and distilled water were compared to analyze the effect of seawater alkalinity. The results indicate that seawater is more appropriate than distilled water due to its alkalinity, obtaining almost 100% cleaning efficiency for the conditions analyzed. This SO_2 reduction meets the limits of SO_x emission control areas (SECA) when operating on heavy fuel oil. These numerical simulations were satisfactory validated with experimental tests. Such data are essential in designing seawater scrubbers and judging the operating cost of seawater scrubbing compared to alternative fuels.

Keywords: Sulphur dioxide, SO_2, scrubbers, CFD

INTRODUCTION

Most medium and large marine engines operate on heavy fuel oil. This is a cheap combustible but contains an important quantity of pollutant substances, especially sulphur. Oxidation of the sulphur in the fuel forms sulphur oxides (SOx) in the exhaust gas, which constitute the major source of acid rain. In order to prevent SOx formation, IMO Annex VI of MARPOL 73/78, Regulations for the Prevention of Air Pollution from Ships, which was ratified and entered into force from 2005, regulates the SOx emissions by setting a maximum limiting value on the fuel sulphur content. This limit has been progressively reduced, from 4.5% to 3.5% from January 1st 2012 and from 3.5 to 0.5% w/w from January 1st 2020. Besides, there are sulphur emission control areas (SECA) with more stringent requirements. So far, using low sulphur content fuels was preferred to scrubbing applications. Nevertheless, exhaust gas cleaning/after-treatment systems have become a promising alternative due to these stricter emission limits and the high price of alternative fuels [1].

Regarding exhaust gas cleaning/after-treatment systems, there are many alkali absorbents such as urea, NaOH, limestone slurry, NaCl, etc. Seawater is a promising solution for marine applications. The main advantages of seawater are the availability and the fact that the acidified effluent can be discharged directly into the sea after a simple neutralization process.

There are some reports about seawater scrubbers available in the literature. For instance, Zhang et al. [2], Oikawa et al. [3] and Williams [4] analyzed seawater wet scrubbers used in power plants. Sun et al. [5] focused on a membrane contactor scrubber and showed that the mass transfer coefficient in seawater is about twice of the NaOH solution with pH 8.35. Darake et al. [6] carried out an experimental study and mathematical modelling of SO_2 removal by seawater in a packed-bed tower. Caiazzo et al. [7] analyzed a seawater spray scrubber operating under marine diesel exhaust conditions and compared seawater and distilled water in order to

elucidate the effect of seawater. Andreansen and Mayer [8] formulated a model to analyze seawater scrubbing, focused on marine engine applications, and concluded that a seawater scrubber is a promising option to low sulphur fuels. Sukheon and Nishida [9] analyzed the effect of seawater under SO_x, particulate matter, CO_2 and NO_x.

In order to expand this literature about seawater scrubbers, the purpose of this paper is to develop a numerical model to analyze SO_2 absorption by seawater. A moving water droplet immersed in a gas medium was analyzed. Both liquid and gas phases were included in the model. The proposed CFD model takes in consideration the fluid motion inside and outside the droplet, heat transfer, chemical reactions and mass diffusion. In order to validate the numerical results with experimental ones, the single droplet model was implemented into a complete spray model.

COMPUTATION OF SO2 ABSORPTION

PHYSICAL AND CHEMICAL DESCRIPTION OF THE PROBLEM

A schematic representation of a seawater scrubber is indicated in Fig. 1. A spray of falling-down droplets encounters a counter-current exhaust gas flow which contains SO_x and other pollutants. Each droplet is exposed to the exhaust gas, and the viscosity between the gas and droplet induce a shear stress. This drag force promotes a vortex motion in the interior of the droplet, indicated in the figure. The droplet velocity tends to decay in the course of movement due to the drag effect. Soon after the gas is in touch with the droplet, a concentration gradient is induced in the interface and SO_2 is transported into the water by mass diffusion. At the same time, chemical dissociation reactions take place.

The model proposed in the present paper analyzes the amount of SO_2 absorbed by a single droplet, with given initial velocity and diameter, falling counter flow with respect to the exhaust gas stream coming from a typical marine engine burning heavy fuel oil. The following assumptions were adopted in order to simplify the problem:

- Axisymmetric flow on both phases.
- The shape of the droplet remains spherical due to surface tension and viscous forces.
- The fluids are Newtonian.
- The flow fields are laminar due to its low Reynolds numbers.
- Phase equilibrium, Henry's law, prevails at the interface.
- Mass diffusion follows Fick's law.

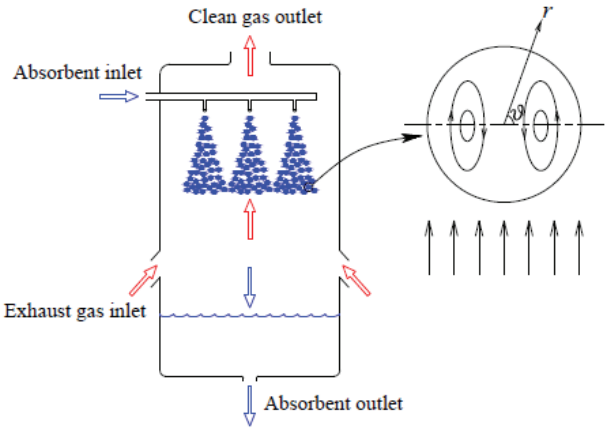

Fig. 1. Schematic representation of the problem

While the average salinity depends on the regional location, the relative amounts of the constituents of seawater are more or less invariant. Many alkaline species are presented in seawater, such as HCO_3^-, CO_3^{2-}, OH^-, HPO_4^{2-}, etc. Between them, the main contribution to alkalinity is by far the bicarbonate ion HCO_3^-. Typical alkaline concentrations are 2400 μmol/kg of H_2O [8, 10, 11].

Inside the droplet, the following reactions take place [8]:

$$SO_2(g) \leftrightarrow SO_2(aq) \quad (1)$$

$$SO_2(aq) + 2H_2O(l) \leftrightarrow HSO_3^-(aq) + H_3O^+(aq) \quad (2)$$

$$HSO_3^-(aq) + H_2O(l) \leftrightarrow SO_3^{2-}(aq) + H_3O^+(aq) \quad (3)$$

$$HCO_3^-(aq) + H_3O^+(aq) \leftrightarrow CO_2(aq) + 2H_2O(l) \quad (4)$$

$$CO_2(aq) \leftrightarrow CO_2(g) \quad (5)$$

Reaction (1) is the dissolution of gaseous SO_2 in water at the liquid-gas interphase, governed by Henry's law:

$$[SO_2(aq)] = p_{SO_2} k_H \quad (6)$$

where p_{SO2} is the partial pressure of SO_2, $[SO_2(aq)]$ is the concentration of SO_2 in the solution and k_H is Henry's constant, expressed as:

$$k_H = k_H^0 e^{\frac{-\Delta H_{soln}}{R}\left(\frac{1}{T}-\frac{1}{T^0}\right)} \quad (7)$$

where k_H^0 is the Henry's constant at the reference state, ΔH_{soln} is the enthalpy of solution, T is the temperature and T^0 is the reference state temperature (298.15 K). A value of k_H^0 = 1.2 mol/(kg atm) and the slope - $\Delta H_{soln}/R$ = 2850 K were employed, Sander [12].

Reaction (2) is the reaction between dissolved SO_2 and water, producing bisulfite. Reaction (3) is the dissociation of bisulfite to sulfite. Reaction (4) is the neutralization of formed bisulfite with the seawater alkalinity. Reactions (2-4) are so fast to assume equilibrium, Andreansen and Mayer [8].

Reaction (5) is the dissolution of CO_2 at the liquid-gas interphase, also governed by Henry's law. A value of k_H^0 = 0.034 mol/(kg atm) and - $\Delta H_{soln}/R$ = 2400 K were employed, Sander [12].

GOVERNING EQUATIONS

As mentioned previously, the fluid motion inside and outside a droplet, heat transfer, chemical reactions and mass diffusion were analyzed. The governing equations consist of the continuity, momentum, energy and species for both liquid and gas phases, Table 1.

Tab. 1. Governing equations

Gas phase	**Continuity**	$\nabla \cdot \overrightarrow{u_g} = 0$
	Momentum	$\frac{\partial(\rho_g \overrightarrow{u_g})}{\partial t} = -\nabla \cdot (\rho_g \overrightarrow{u_g}\overrightarrow{u_g}) - \nabla p_g - \nabla \cdot \tau_g$
	Energy	$\frac{\partial(\rho_g c_{pg} T)}{\partial t} + \nabla \cdot (\rho_g \overrightarrow{u_g} c_{pg} T) = \nabla \cdot (k_g \nabla T)$
	Species	$\frac{\partial C_i}{\partial t} = -\nabla \cdot (C_i \overrightarrow{u_g}) - D_g \nabla^2 C_i + R_i$
Liquid phase	**Continuity**	$\nabla \cdot \overrightarrow{u_l} = 0$
	Momentum	$\frac{\partial(\rho_l \overrightarrow{u_l})}{\partial t} = -\nabla \cdot (\rho_l \overrightarrow{u_l}\overrightarrow{u_l}) - \nabla p_l - \nabla \cdot \tau_l$
	Energy	$\frac{\partial(\rho_l c_{pl} T)}{\partial t} + \nabla \cdot (\rho_l \overrightarrow{u_l} c_{pl} T) = \nabla \cdot (k_l \nabla T)$
	Species	-

In the equations above, the subscript i shown in the species equations represents SO_2, HSO_3^-, H_3O^+, SO_3^{2-}, HCO_3^- or CO_2. C is the concentration, D the mass diffusivity, c_p the specific heat, and R a source which models the chemical reactions.

A reference frame which moves with the droplet was employed. A free-stream velocity was imposed as inlet boundary condition. The drag force decelerates the relative velocity between the droplet and gas, and this was implemented in the numerical model adjusting the free-stream velocity at each time step. The deceleration is given by:

$$\frac{du_\infty(t)}{dt} = \frac{F_{drag}}{\rho_l \pi D^3 / 6} + g \tag{8}$$

where u_∞ is the free-stream velocity, F_{drag} the drag force, ρ_l the seawater density, ρ_g the gas density and D the droplet diameter.

The free-stream velocity after a time step Δt is given by:

$$u_\infty(t + \Delta t) = u_\infty(t) + \Delta t \frac{du_\infty(t)}{dt} \tag{9}$$

Heat transfer between the droplet and gas was considered. Inside the droplet, the energy equation was solved until the evaporation temperature was reached. From this temperature, the computational grid was regenerated at every time step to account for droplet diameter reduction due to evaporation. The rate of change of the droplet mass, which is equivalent to the rate of evaporated mass, is obtained from a heat balance:

$$hA(T_e - T_g) = \frac{dm}{dt} h_{fg} \tag{10}$$

where T_e is the evaporation temperature, T_g the gas temperature, h_{fg} the latent heat of evaporation, A the surface and h the heat transfer coefficient, given by the Ranz-Marshall equation [13]:

$$\frac{hD}{k} = 2 + 0.6\,\mathrm{Re}^{1/2}\,\mathrm{Pr}^{1/3} \tag{11}$$

where D is the droplet diameter, k the thermal conductivity, *Re* the Reynolds number and *Pr* the Prandtl number.

As initial conditions, zero velocity was imposed to the liquid phase and free-stream velocity to the gas phase. The free-stream velocity was also imposed as boundary condition. A zero SO_2 concentration was imposed to the liquid phase. Regarding the gas phase, initial SO_2 concentrations between 500 and 1000 ppm were studied, corresponding to typical values for exhaust gas from marine engines operating on fuel oil [14, 15].

CFD MODEL

The computational mesh is indicated in Fig. 2. The grid size is uniform in the tangential direction, with $\Delta\theta = 4^o$. In the radial direction the mesh is finer inside the droplet and near the interface. The domain size was 15 droplet radii from the droplet center. Several tests were performed in order to determine the adequate extent of the domain in such a way as to eliminate any potential effects of the outer boundaries on the flow close to the droplet. As mentioned previously, this grid was regenerated at every time step to account for the droplet reduction.

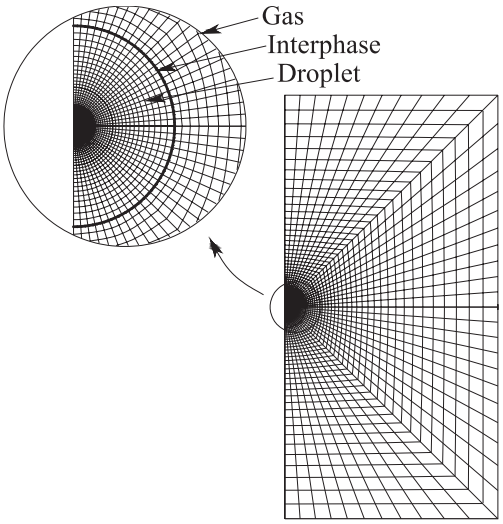

Figure 2. Computational mesh.

The problem was simulated using the open software OpenFOAM (Open Field Operation and Manipulation).

This software was chosen because it allows total manipulation of the code. A new OpenFOAM solver was developed for the presented study. C++ programming language was employed to write this new solver.

OpenFOAM is based on the finite volume method. The pressure-velocity coupling was treated using the PISO (Pressure Implicit Splitting of Operators) procedure. The equations were discretized by the QUICK interpolation and the temporal treatment was solved by an implicit method. The solution was checked for refinement sensibility on both mesh size and time step.

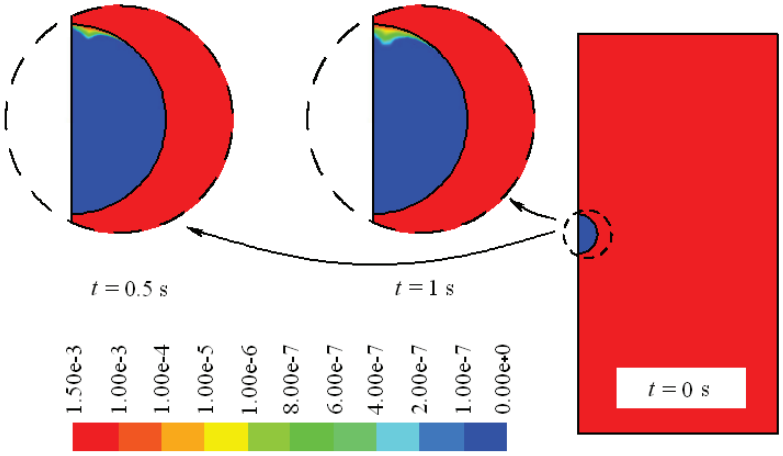

Figure 5. Mass fraction of SO2.

RESULTS

Fig. 3 shows the velocity field for 600 ppm SO_2 concentration (i.e., 0.00133 kg /kg of H_2O), alkaline concentration 2400 µmol/kg of H_2O (*i.e.*, 0.000146 kg/kg of H_2O), free stream velocity 2 m/s and initial droplet of 1 mm diameter. As can be seen, a vortex is created inside the droplet. Figs. 4 and 5 indicate the mass fraction of HCO_3^- and SO_2 respectively, for 0.5 and 1 s. These figures indicate that SO_2 is initially at the droplet surface and then the internal vortex transports SO_2 to the core of the droplet. HCO_3^- is consumed first at the interphase and then at the core of the droplet.

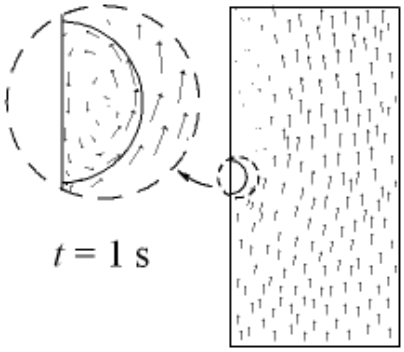

Figure 3. Velocity field, → 2 m/s.

EXPERIMENTAL VALIDATION

The accuracy of CFD models applied to marine engines was previously validated in simulations of the scavenging process [16-17], combustion [19] and NO_x reduction methods [19-21]. Nevertheless, it is important to check the accuracy of the CFD model proposed in the present paper, i.e., SO_x reduction. To this end, the results were compared with experimental tests obtained by Caiazzo et al. [7].

These authors analyzed a seawater spray scrubber which can be numerically reproduced since the liquid flow is composed by a set of independent droplets. In their experimental setup, Caiazzo et al. [7] employed a compressor to blow air and a heater to reach 250 °C. A stream of air with SO_2 was employed and water was injected countercurrent in a 180 mm diameter and 1880 mm height tube. The SO_2 capture efficiency was calculated by comparing the outlet SO_2 concentration to the inlet SO_2 concentration. A fast camera was employed to measure the droplet diameter. In the experimental tests, a fixed gas flow rate of 40 m3/h was employed. Three different inlet SO_2 concentration levels were tested, 500, 700 and 900 ppm. The water flow rate was varied in the range 0.06-0.4 m^3/h corresponding to liquid-to-gas ratios in the range of 1-10x10^{-3}, common in the marine field [14-15]. Both water and seawater were compared.

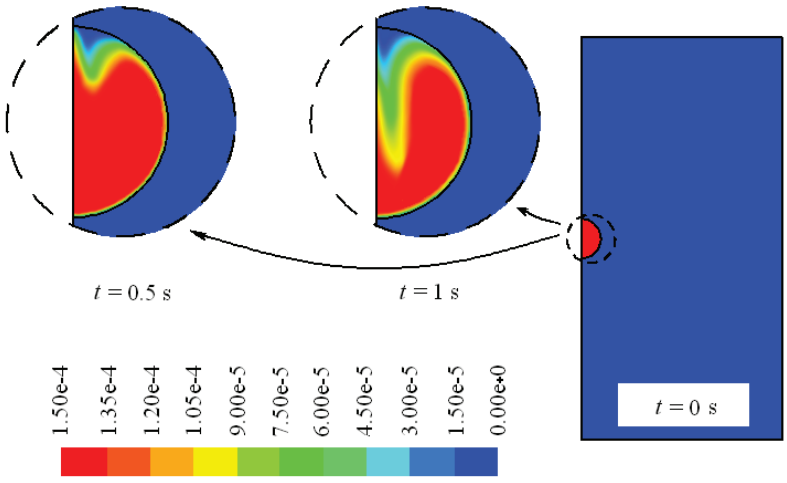

Figure 4. Mass fraction of HCO_3^-.

Fig. 6 indicates the desulfurization results obtained with distilled water. The desulfurization efficiency increases with the liquid flow rate. As can be seen, numerical results indicate a lower desulfurization efficiency than experimental setups. As original distilled water had negligible alkalinity, after pouring and mixing in the tank

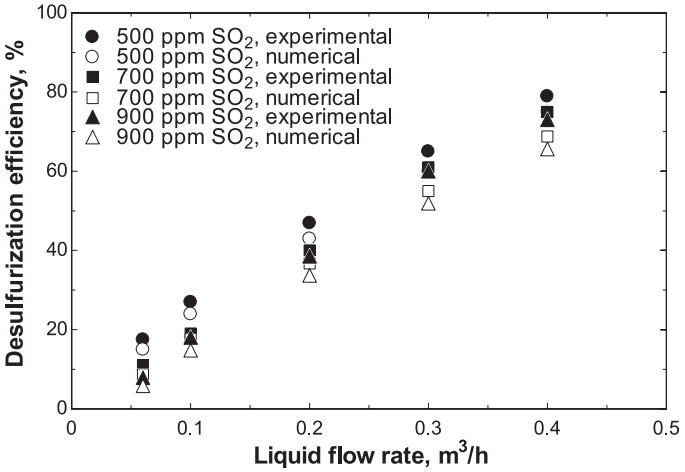

Fig. 6. Numerical and experimental desulfurization efficiency results. Distilled water. Gas flow rate 40 m³/h

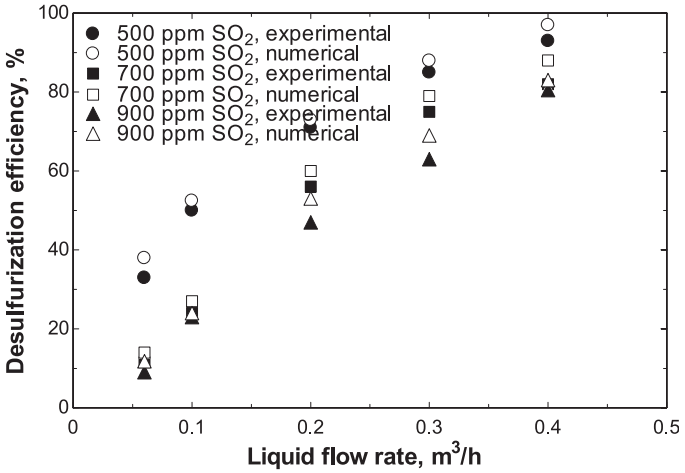

Fig. 7. Numerical and experimental desulfurization efficiency results. Seawater water. Gas flow rate 40 m³/h

this water contaminates with seawater residue in the tank and/or in the lines left from previous experiments, Caiazzo et al. [7].

Fig. 7 illustrates the desulfurization results obtained with seawater under the same conditions. As expected, seawater is more efficient than distillated water due to the alkalinity. Fig. 8 illustrates the desulfurization results for seawater under 60 m³/h gas flow rate.

Fig. 9 illustrates a summary where all the data are represented in a parity plot. A satisfactory concordance was obtained.

CONCLUSIONS

A numerical investigation was developed on SO_2 capture by means of seawater. The internal circulation, droplet deceleration, evaporation, mass and heat exchange were modeled. The transport equations were solved for both liquid and gas phases on a non uniform computational grid, which was regenerated at every time step to account for droplet diameter reduction.

The numerical results were compared with experimental tests, giving a satisfactory correspondence. This model is very useful when designing new models of seawater scrubbers.

Almost 100% of SO_2 capture efficiencies were obtained, which indicates that SO_2 scrubbing by seawater is a promising solution for marine applications. It allows to use heavy fuel oil instead of expensive low sulphur fuels such as Marine Diesel Oil or Marine Gas Oil.

ACKNOWLEDGEMENTS

The authors would like to express their gratitude to "Talleres Pineiro, S.L.", sale and repair of marine engines.

REFERENCES

1. Lamas, M.I.; Rodríguez, C.G.; Telmo, J.; Rodríguez, J.D. Numerical analysis of emissions from marine engines using alternative fuels. Submitted to Polish Maritime Research.

2. Zhang, D.N.; Chen, Q.Z.; Zhao, Y.X.; Maeda, Y.; Tsujino, Y. Stack gas desulfurization by seawater in Shanghai. Water, Air & Soil Pollution, vol. 130, pp. 271-276, 2001.

3. Oikawa, K.; Yongsiri, C.; Takeda, K.; Harimoto, T.

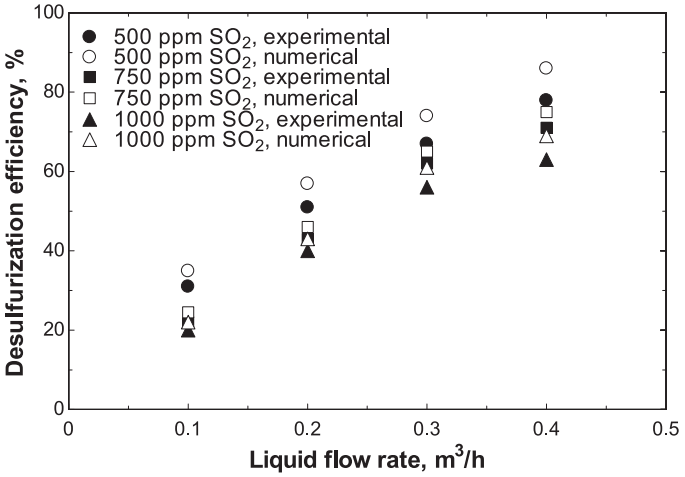

Fig. 8. Numerical and experimental desulfurization efficiency results. Seawater water. Gas flow rate 60 m³/h

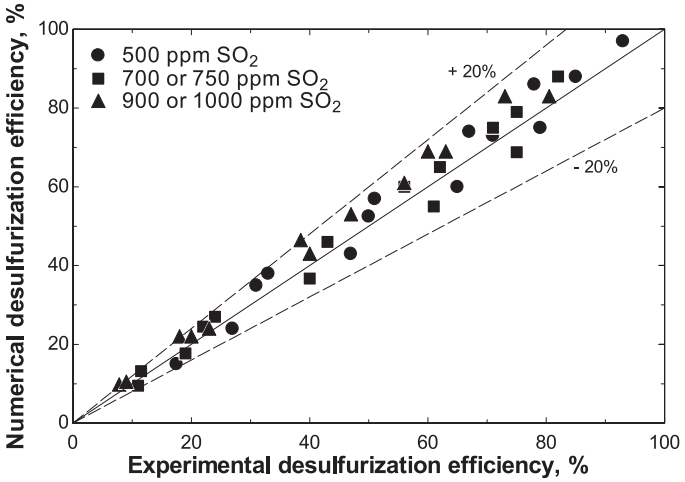

Fig. 9. Comparison between numerical and experimental results

Environmental Progress, vol. 22, pp. 67-73, 2003.

4. Williams, P.J. Use of seawater as makeup water for wet flue gas desulfurization systems. EPRI-DOE-EPA Combined Utility Air Pollution Control Symphosium, August 16-20. Atlanta, Georgia, USA, 1999.

5. Sun, X.; Meng, F.; Yang, F. Application of seawater to enhance SO2 removal from simulated flue gas through hollow fiber membrane contactor. Journal of Membrane Science, vol. 312, pp. 6-14, 2008.

6. Darake, S.; Rahimi, A.; Hatamipour, M.S.; Hamzeloui, P. SO2 removal by seawater in a packed-bed tower: experimental study and mathematical modelling. Separation Science and Technology, vol. 49, pp. 988-998, 2014.

7. Caiazzo, G.; Langella, G.; Miccio, F.; Scala, F. An experimental investigation on seawater SO2 scrubbing for marine application. Environmental Progress & Sustainable Energy, vol. 32, pp. 1179-1186, 2013.

8. Andreasen, A.; Mayer, S. Use of seawater scrubbing for SO2 removal from marine engine exhaust gas. Energy & Fuels, vol. 21, pp. 3274-3279, 2007.

9. Sukheon, A.; Nishida, O. New application of seawater and electrolyze seawater in air pollution control of marine diesel engine. JMSE International Journal, Series B: Fluids and Thermal Engineering, vol. 46, pp. 206-213, 2003.

10. Sverdrup, H. U.; Johnson, M. W.; Fleming, R. H. The Oceans Their Physics, Chemistry, and General Biology; Prentice-Hall: New York, 1942.

11. Dickson, A. G.; Goyet, C., Eds.; Handbook of Methods for the Analysis of the various Parameters of the Carbon Dioxide System in Sea Water, Version 2, ORNL/CDIAC-74; U.S. Department of Energy: Washington, DC, 1994.

12. Sander, R. Henry's Law Constants. In NIST Chemistry Webbook; NIST Standard Reference Database Number 69; Linstrom P. J., Mallard W. G., Eds.; National Institute of Standards and Technology: Gaithersburg, MD, 2005.

13. Ranz, W.E.; Marshall, W.R. Evaporation from drops, Chemical Engineering Progress, vol. 48, pp. 141-146, 1952.

14. Kuiken, K. (2008): Diesel engines for ship propulsion and power plants from 0 to 100000 kW. 1st Edition. The Netherlands: Target Global Energy Training.

15. Woodyard, D. Pounder's marine diesel engines and gas turbines. 9th Edition. Oxford. Elsevier, 2009.

16. Lamas, M.I.; Rodríguez, C.G. CFD analysis of the scavenging process in the MAN B&W 7S50MC two-stroke diesel marine engine. Journal of Ship Research, vol. 56(3), pp. 154–161, 2012.

17. Lamas, M.I.; Rodríguez, C.G.; Rebollido, J.M. Numerical model to study the valve overlap period in the Wärtsilä 6L46 four-stroke marine engine. Polish Maritime Research, vol.18, pp. 31-37, 2012.

18. Lamas, M.I.; Rodríguez, C.G.; Rodríguez, J.D.; Telmo, J. Numerical analysis of several port configurations in the Fairbanks-Morse 38D8-1/8 opposed piston marine engine. Brodogradnja, vol. 66, no. 1, pp. 1-11, 2015.

19. Lamas, M.I.; Rodríguez, C.G. Numerical model to study the combustion process and emissions in the Wärtsilä 6L 46 four-stroke marine engine. Polish Maritime Research, vol. 20, pp. 61-66, 2013.

20. Lamas, M.I.; Rodríguez, C.G.; Aas, H.P. Computational fluid dynamics analysis of NOx and other pollutants in the MAN B&W 7S50MC marine engine and effect of EGR and water addition. International Journal of Maritime Engineering, vol. 155, Part A2, pp. A81-A88, 2013.

21. Lamas, M.I.; Rodríguez, C.G.; Rodríguez, J.D.; Telmo, J. Internal modifications to reduce pollutant emissions from marine engines. A numerical approach. Journal of Naval Architecture and Marine Engineering, vol. 5(4), pp. 493-501, 2013.

22. Lamas, M.I.; Rodríguez, C.G.; Rodríguez, J.D.; Telmo, J. Computational fluid dynamics of NOx reduction by ammonia injection in the MAN B&W 7S50MC marine engine. International Journal of Maritime Engineering, vol. 156, Part A3, pp. A213-A220, 2014.

CONTACT WITH THE AUTHOR

M.I. Lamas

Escuela Politécnica Superior
C/Mendizábal s/n. 15403Ferrol
A Coruña.

e-mail: isabellamas@udc.es

SPAIN